J Appl Electrochem (2008) 38:1637–1646
DOI 10.1007/s10800-008-9610-7

ORIGINAL PAPER

Degradation of oxygen-depolarized Ag-based gas diffusion electrodes for chlor-alkali cells

S. Siracusano · T. Denaro · V. Antonucci · A. S. Aricò · C. Urgeghe · F. Federico

Received: 15 June 2007 / Accepted: 20 May 2008 / Published online: 17 June 2008

Abstract Oxygen-depolarized cathodes consisting of gas-diffusion electrodes (GDEs) for electrolysis in a chlor-alkali cell at 90 °C were studied. The electrode design was based on a carbon-free catalyst and comprised of a mixture of micronized silver particles, a small amount of Hg and PTFE binder. The cathodes were investigated by electrochemical measurements, and surface and morphological analyses before and after different operation times in chlor-alkali cells. Electrode stability was investigated by life-time tests. The surface properties of gas diffusion electrodes were studied for both fresh and used cathodes by X-ray photoelectron spectroscopy (XPS). Transmission (TEM) and scanning electron microscopy (SEM-EDX) were used to investigate morphology. The bulk of gas diffusion electrodes was studied by X-ray diffraction (XRD) and thermogravimetric analysis (TG-DSC). At least two main degradation processes that occur on different time-scales were identified and attributed to segregation and loss of the second metal at the interface and a decrease in the hydrophilic properties with time. Furthermore, an increase in the precipitation of compounds from the reaction process also decreased performance by the occlusion of reaction pores.

S. Siracusano (✉) · T. Denaro · V. Antonucci · A. S. Aricò
CNR-ITAE, Via Salita Santa Lucia Sopra Contesse 5,
Messina 98126, Italy
e-mail: siracusano@itae.cnr.it

C. Urgeghe · F. Federico
Industrie De Nora S.p.A., via Bistolfi 35, Milan 20134, Italy

Keywords Oxygen reduction, cathode · Chlor-alkali electrolysis · Gas diffusion electrode · Carbon-free catalyst

1 Introduction

Chlorine and caustic soda, obtained by the electrolysis of an aqueous solution of sodium chloride, are products of the chlor-alkali electrochemical process. Total cell reaction proceeds through the following anodic and cathodic half-cell reactions:

$$2Cl^- \rightarrow Cl_2 + 2e^- \qquad E = 1.358\ V \quad vs.\ NHE \tag{1}$$

In alkaline solutions,

$$2H_2O + 2e^- \rightarrow 2OH^- + H_2 \qquad E = -0.828\ V \quad vs.\ NHE \tag{2}$$

Therefore, the overall reaction is:

$$2H_2O + 2Cl^- \rightarrow Cl_2 + 2OH^- + H_2 \qquad E = -2.186\ V \tag{3}$$

The thermodynamic potential difference ΔE (decomposition voltage) of total electrode reactions is approximately 2.2 V.

The main drawback of chlor-alkali electrolysis (3) is high power consumption, about 4 kA m^{-2}@ 3 V [1]. Therefore, in order to improve the process, it is necessary to reduce energy consumption. In the early 1980s, chlor-alkali cells utilizing air cathodes were developed at ELTECH System Co. [2, 3]. The use of these Gas Diffusion Electrodes (GDEs) was introduced as a feasible technological approach for the reduction of power consumption in the chlor-alkali membrane cell process.

The substitution of traditional hydrogen-evolving cathodes with an oxygen-consuming GDE results in the formation of caustic and chlorine without hydrogen:

$$\text{Anode reaction}: 2Cl^- \rightarrow Cl_2 + 2e^- \quad E = +1.358\ \text{V} \quad \text{vs. NHE} \qquad (1)$$

$$\text{Cathode reaction}: 2H_2O + O_2 + 4e^- \rightarrow 4OH^- \quad E = +0.401\ \text{V} \quad \text{vs. NHE} \qquad (4)$$

$$\text{Overall reaction}: 2H_2O + O_2 + 2Cl^- \rightarrow Cl_2 + 4OH^- \quad E = 0.957\ \text{V} \qquad (5)$$

The equilibrium potential of reactions (2) and (4) is −0.82 and +0.40 V versus NHE, respectively. Thus, the equilibrium potential of the oxygen reduction reaction versus NHE (4) is about 1.2 V higher than that of the hydrogen evolution reaction (2). Therefore, replacing hydrogen-evolving cathodes with oxygen cathodes significantly reduces thermodynamic cell voltage and leads to an energy saving of 30–40% [4–6].

The first GDE structures were based on silver catalyst particles supported on active carbon [7, 8]. These catalysts were affected by significant deactivation phenomena:

- Electrode flooding, due to a progressive loss of hydrophobicity and the intrusion of the catholyte into electrode pores. This is favoured by the differential pressure existing between the gas and liquid sides of the electrode. Progressive corrosion of both carbonaceous components and the silver catalyst, followed by silver redistribution
- Sensitivity to uncontrolled shut-down.

All these reasons suggested attention be concentrated on a different type of electrode design based on a carbon-free catalyst.

Catalysts used in this study were based on a mixture of micronized silver particles and PTFE binder. The silver particles showed a very uniform size distribution and contained a limited amount of second metal (i.e. Hg) that was introduced to increase their stability to corrosion, as demonstrated by the RDE analysis of catalyst powder [9].

The purpose of the present study was to investigate the cathodic properties of oxygen reduction on gas-diffusion electrodes by electrochemical measurements, and surface and morphologic analyses. Attention was focused on deactivation phenomena involving this type of GDE configuration. In this study, we compared fresh gas diffusion electrodes to electrodes tested at different times in a chlor-alkali cell. Electrode stability was investigated with life-time tests. The surface of the gas diffusion electrodes was observed and analyzed for both fresh and used cathodes by scanning electron microscopy and X-ray photoelectron spectroscopy. The bulk of the gas diffusion electrodes was investigated by X-ray diffraction and thermogravimetric analysis.

2 Experimental

Catalysts used for the cathodic reaction were based on a mixture of silver particles containing a limited amount of Hg (comprised in the range 0.5–10% by weight) and PTFE binder. Electrodes tested in this study were composed of an Ag net loaded with a 1 kg m^{-2} catalyst. With respect to what is considered optimum in current literature [10], a large excess of metal loading was used in this study to avoid any degradation of the support after prolonged operation, thus focusing attention on phenomena occurring mainly at the surface of the electrocatalyst. The electrodes were prepared by a powder roller of PTFE and a silver–mercury alloy obtained by a co-precipitation process and, subsequently, reduced electro-chemically, according to the patent of Janowitz et al. [11]. In this investigation, the following samples obtained from the same electrode roll were analysed: GDE-fresh (before electrochemical characterization), GDE-1 (after a 50-h time- study), GDE-2 (after a 145-h time-study), and GDE-3 (after a 526-h time-study). A standard chlor-alkali electrolyser (300 g/L NaCl; 90 °C) was used. A sodium chloride solution was fed to the anode, to produce chlorine gas (1), whereas oxygen was fed to the cathode (2). The sodium hydroxide formed at the cathode was maintained separate from the sodium chloride solution present in the anodic compartment by a membrane made of a perfluorinated polymer containing anionic groups (i.e. DuPont N324). A more detailed description of the electrolyser and a design of this type of cell is illustrated in the patent EP1362133 [1]. Electrochemical deactivation phenomena were monitored by chrono-amperometric tests at 3 and 4 kA m^{-2}. The geometrical electrode surface was 0.16 m^2. Cell resistance was determined and monitored as a function of time by using the current interruption method. Morphology was investigated by using SEM-EDX (FEI XL 30)_instruments. Structural analysis was done by X-ray diffraction (Philips X'Pert, diffractometer, Cu Kα source).

To investigate the surface chemical composition of gas-diffusion electrodes, XPS analysis was performed using a PHI 5800-01 spectrometer with an Al Kα monochromatic source. An Ar^+ sputtering procedure was used in order to obtain a qualitative depth-profile of electrode composition. Thermogravimetric analysis of gas diffusion electrodes was carried out by a Netzesch STA 409 Cell analyser. The thermal analysis yielded information about

bulk composition with regard to PTFE and Ag content. Transmission Electron Microscopy (FEI CM 12) was used to obtain qualitative information on the degree of hydrophobicity at the reaction pores.

3 Results and discussion

The variation of cell potential as a function of operational time under constant electrochemical conditions (3 and 4 kA m^{-2}, 90 °C, NaOH 33% w/w) is shown in Fig. 1 for the first 120 h. A significant variation in cell potential is observed during the first period of operation, whereas only small changes are observed after prolonged operation. No relevant modifications in electrochemical behaviour were observed from 120 to 526 h (not shown). Previous electrochemical studies have assigned an increase in cell potential versus time primarily to the oxygen reduction process in gas diffusion electrodes (4), which represents the rate determining step for the overall process [14].

A very low overpotential at a current density of 4 kA m^{-2} was observed for the chlorine evolution (Eq. 1) in half-cell experiments [12, 13]. Previous studies reported no change in the anodic overpotential in a time-test of more than 2 years at a current density of 4 kA m^{-2} [12].

A significant loss of potential in these electrochemical devices occurs by the effect of the ohmic drop caused by the polymer membrane (about 400 mV at 4 kA m^{-2}); yet, according to cell resistance measurements (not shown), the voltage loss due to ohmic resistance does not significantly increase with time.

The cell used in the present study demonstrated excellent stability during uncontrolled shut-down conditions (normal frequency 0.02 h^{-1}, maximum frequency 0.05 h^{-1}, during normal operation). The curve fitting shows that in the first 120 h of operation, two main degradation phenomena occur on different time-scales. A dramatic increase in cell potential is observed at low operational times (up to 40 h) that overlays with a smooth decay after more than 40–50 h. The curve fitting related to an increase in overpotential (η) with operation time is mathematically expressed by Eqs. 6 and 7

$$\eta_1 = 2.16157 - 0.10255 \times e^{-\frac{t}{6.766192}} + 0.00029 \times t \quad (6)$$

$$\eta_2 = 1.99568 - 0.07608 \times e^{-\frac{t}{5.39529}} + 0.00023 \times t \quad (7)$$

The first phenomenon suitably fits a naperian exponential term with a negative pre-exponential factor and reflects a strong deactivation process. The second process is associated with a progressive decay approximated by a linear function. The first phenomenon is more significant and its effect also influences long-term electrochemical behaviour even if to a lesser extent than initially observed.

This behaviour was quite reproducible, indicating that it is associated with physico-chemical changes in electrode properties at the interface. To have a complete picture of the electrode changes, both bulk and surface analyses were carried out on electrodes discharged after specific operation times.

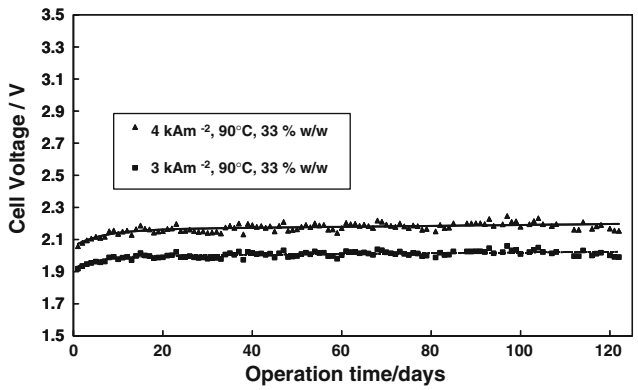

Fig. 1 Cell voltage of chlor-alkali cell versus time. Lines represent curve fitting according to Eq. 5 (—) and 6 (- - -)

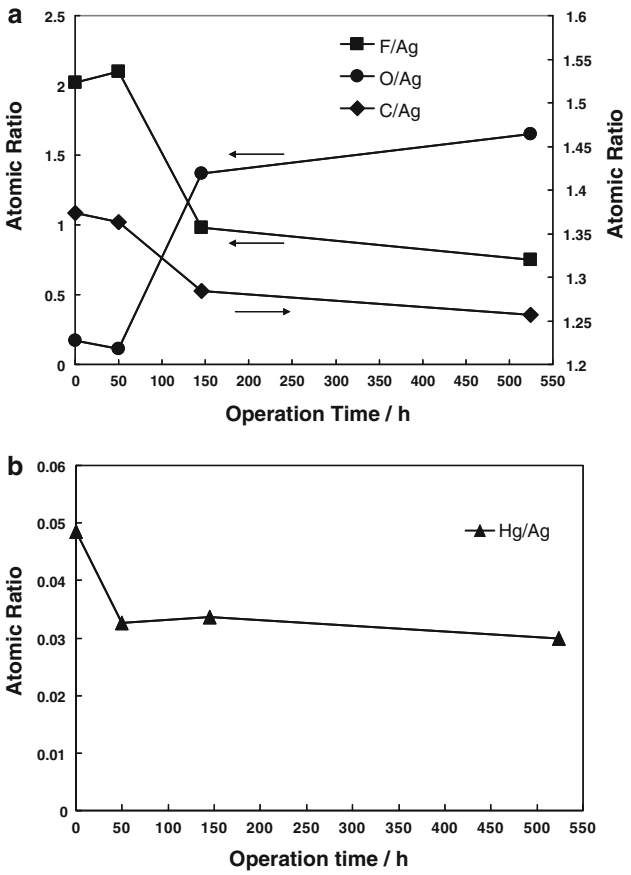

Fig. 2 (**a**, **b**) EDX analysis at GDE-fresh, GDE-1 (50 h), GDE-2 (145 h) and GDE-3 (526 h). Atomic ratios of different elements

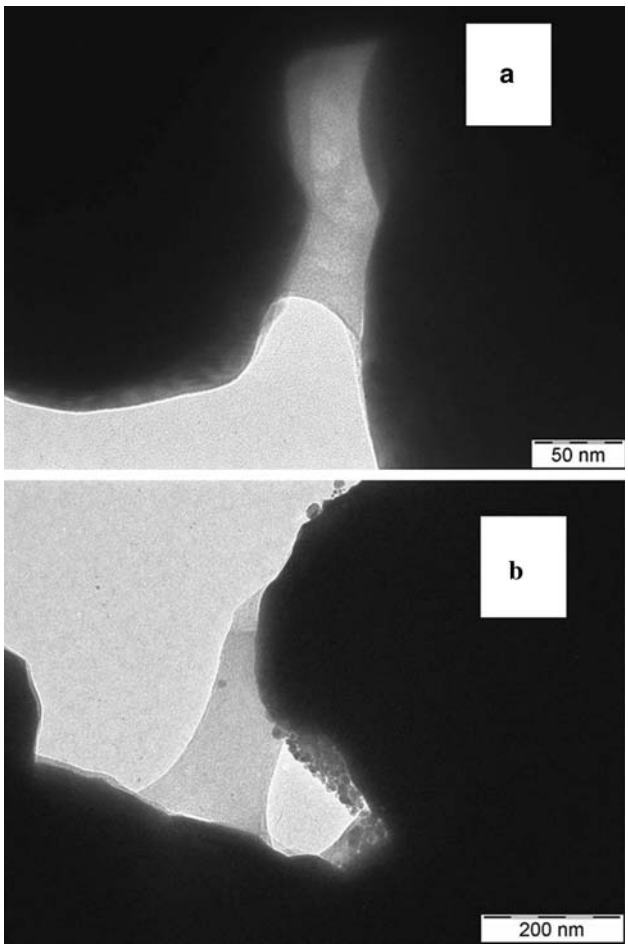

Fig. 3 TEM images of GDE-fresh (**a**) and GDE-2 (**b**)

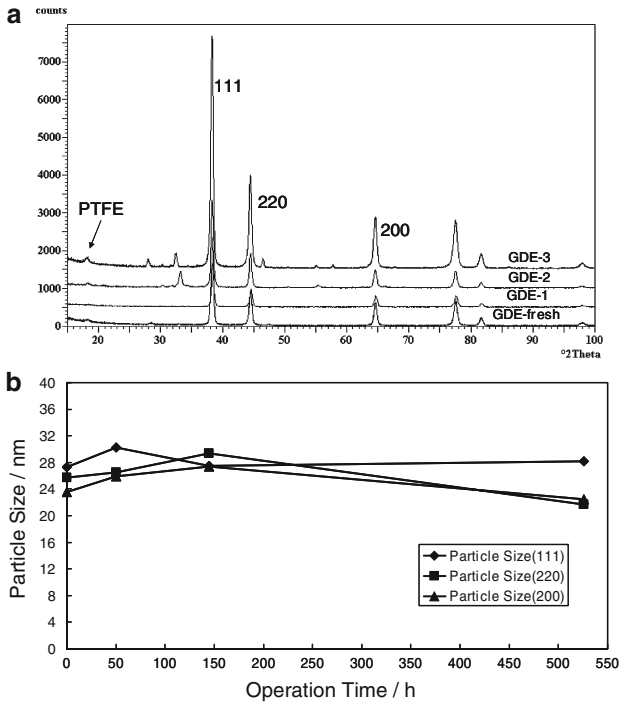

Fig. 4 (**a**) X-ray diffraction patterns of GDE-fresh, GDE-1, GDE-2 and GDE-3 electrodes. (**b**) Comparison of the values of particle size of main peaks of Ag fcc crystalline structure i.e. 111, 220 and 200 reflections

Figure 2 shows a comparison of different atomic ratios for the GDE-fresh, GDE-1, GDE-2, and GDE-3 samples as derived from SEM-EDX. The atomic ratio of F/Ag and C/Ag decreased with time whereas the atomic ratio of O/Ag increased. This means that hydrophobicity decreased and the amount of hydroxides increased. A drastic decrease in the Hg/Ag ratio was observed in the first 50 h.

The decrease in hydrophobicity was further investigated by TEM analysis (Fig. 3a–b). It was observed that catalyst pores were properly coated with the PTFE polymer in the fresh electrode. Upon operation, this PTFE coating is partially lost due to progressive flooding of the electrode surface.

In Fig. 4a–b, XRD patterns and the values of particle size for the main Ag peaks, i.e. 111, 220, and 200, are reported. There was no significant change in the particle size of the catalysts at different intervals of operation. This indicates that the degradation of electrodes is not associated with electrochemical sintering of the catalysts. In effect, the raw particle size of Ag is quite large, about 25 nm, whereas electrochemical sintering phenomena involving dissolution and reprecipitation in fuel cell catalysts used in the oxygen reduction process are usually associated with small particle sizes (<10 nm) [15].

Figure 5 shows Ag 3d and Hg 4f XPS spectra of GDE-fresh, before and after sputtering. After sputtering, the binding Energy (B.E.) of Ag 3d does not change, whereas a shift at lower B.E. values is observed for Hg 4f. This reveals that Hg is partially oxidised on the surface, whereas it is suitably alloyed in the inner layer. From the comparison of peak intensities before and after sputtering, it seems that the amount of Ag decreases from the inner to outer layers, whereas Hg increases. If one combines information about the electronic properties of Hg and its surface enrichment caused by segregation (see below), it appears that Hg is partially lost from the surface during the first hours of operation. This speculation is confirmed below by the XPS and EDX analyses carried out at different operation times.

Figure 6 shows F 1 s and C 1 s XPS spectra of GDE-fresh, before and after sputtering. The peaks of fluorine and carbon decreased after sputtering and significantly shifted to lower B.E. values. This indicates degradation of the PTFE binder by the effect of Ar^+ ions with a consequent change of B. E. and, possibly, a loss of the insulating (charging) effect.

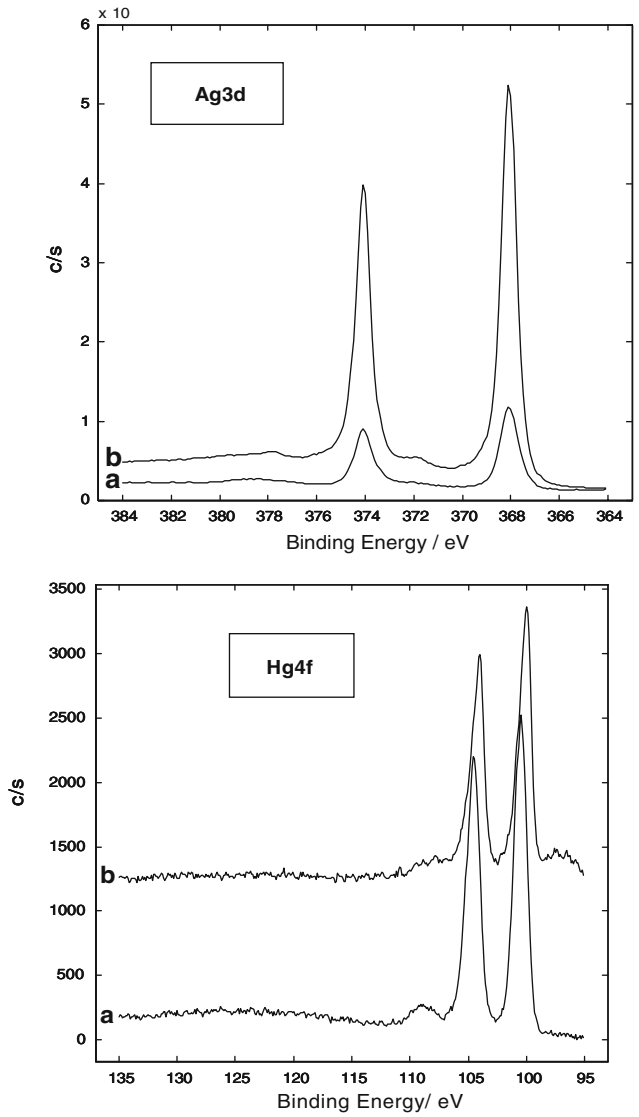

Fig. 5 Ag 3d and Hg 4f XPS spectra of GDE-fresh, before (**a**) and after (**b**) sputtering

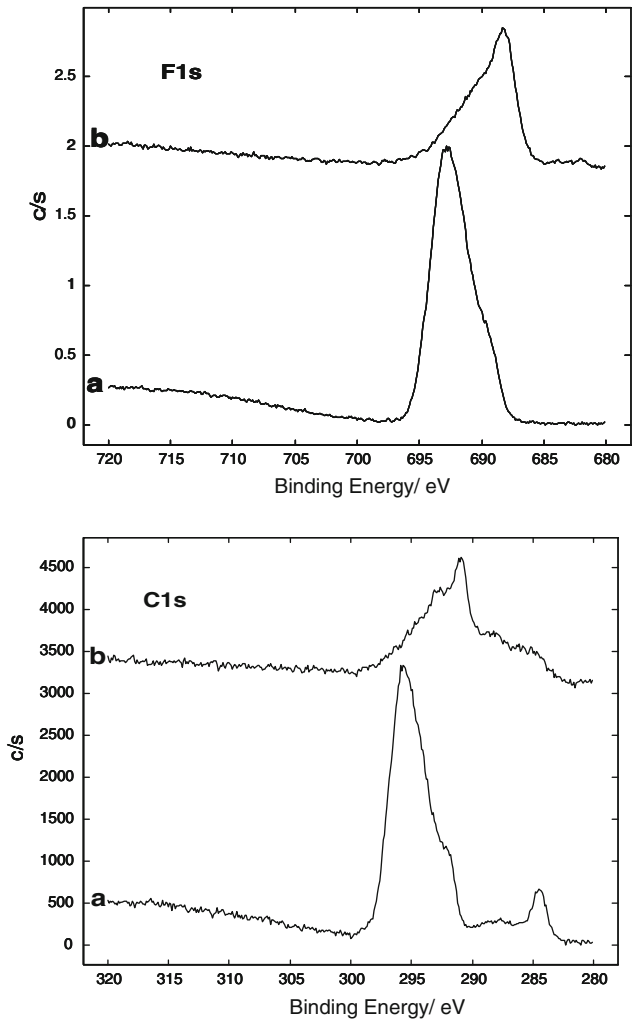

Fig. 6 F 1 s and C 1 s XPS spectra of GDE-fresh, before (**a**) and after (**b**) sputtering

Figure 7 shows Ag 3d and Hg 4f XPS spectra of GDE-1 discharged after 50 h of operation, before and after sputtering. After sputtering, the peak of silver increased, whereas the Hg 4f did not change. By comparing these results to those of fresh electrodes and taking into account the EDX analysis, it appears that significant Hg loss occurs during the first 50 h; subsequently, Hg dissolution proceeds at a lower rate than at the beginning of operation. From sputtering results, we may conclude that the Hg distribution content in the inner layers is homogeneous.

Figure 8 shows C1 s and F1 s XPS spectra of GDE-1 (50 h), before and after sputtering. After sputtering the C1 s signal at high B.E. values associated with PTFE (292 eV) and the F1 s signal shifted toward lower binding energies as observed above. A comparison of fresh electrodes to GDE-1 showed the amount of adventitious carbon (284.6 eV) was significant due to an increased uptake of carbon compounds from the environment.

Figure 9 shows Cl 2p and Na 1 s XPS spectra of GDE-1, before and after sputtering. A low Cl 2p signal indicates that there is no significant precipitation of AgCl after 50 h; the Na 1 s signal does not change significantly in intensity after sputtering. The shift is attributed to a charging effect. It is concluded that sodium hydroxides solidify in the catalyst pores during the electrochemical process.

XPS analysis was also carried out on electrodes discharged after 145 and 526 h of operation. The results of Ag 3d and Hg 4f were qualitatively similar to those observed after 50 h operation. The C1 s and F1 s profiles were somewhat different from that in electrodes tested for 50 h. Figure 10 shows the C 1 s and F 1 s XPS spectra of GDE-2 (145 h), before and after sputtering. After sputtering, carbon and fluorine signals associated with PTFE decreased due to degradation. In this sample, it was observed that adventitious carbon peak (284.6 eV) prevailed with respect

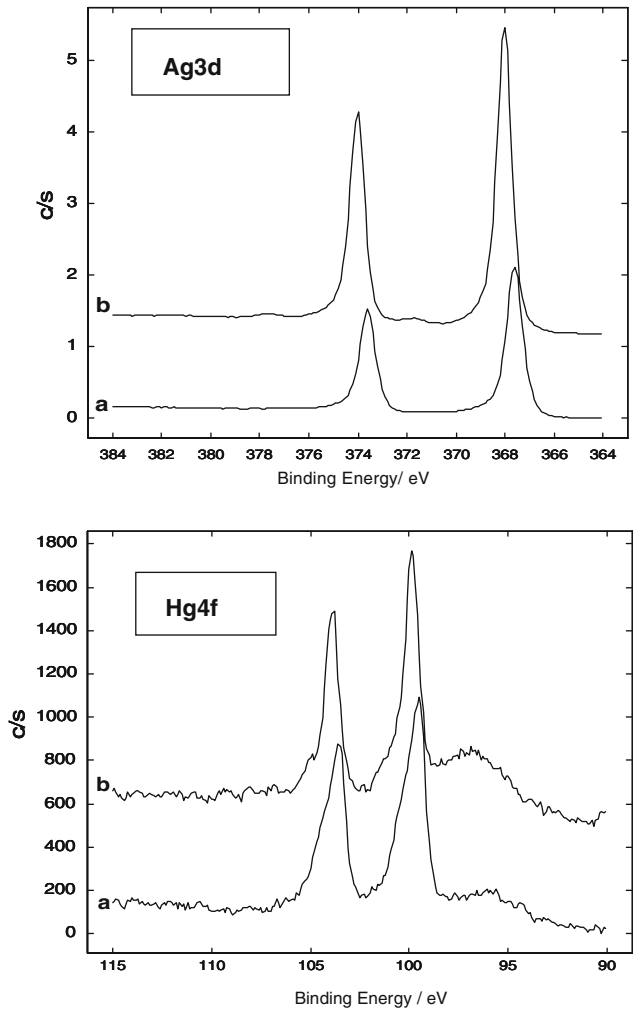

Fig. 7 Ag 3d and Hg 4f XPS spectra of GDE-1 (50 h), before (**a**) and after (**b**) sputtering

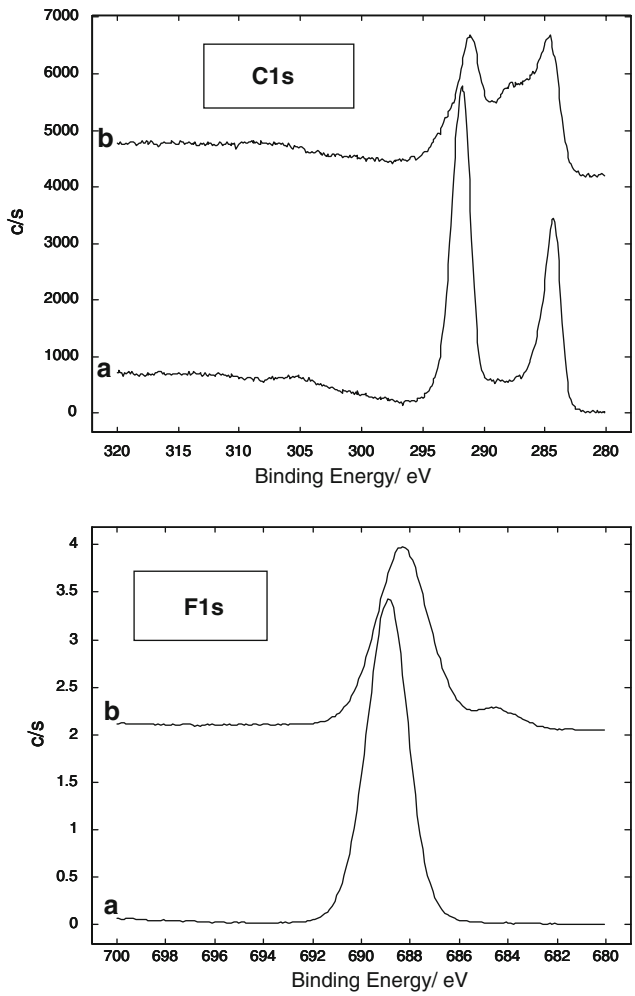

Fig. 8 C 1 s and F 1 s XPS spectra of GDE-1 (50 h), before (**a**) and after (**b**) sputtering

to the C1 s signal associated with PTFE (292 eV). This is due to a large uptake of contaminants from the environment after prolonged electrochemical operation. Figure 11 shows Cl 2p and Na 1 s XPS spectra of GDE-2 (145 h), before and after sputtering. After sputtering, Cl 2p decreased, whereas Na 1 s increased. Both AgCl and sodium hydroxide species precipitated in the pores. It seems that sodium hydroxide precipitation in the inner layers is more significant than that of AgCl.

The surface characteristics of GDE-3 (526 h) were similar to those of GDE-2 (145 h). This is in agreement with the absence of any significant variation in electrochemical properties after 120–150 h (not shown).

A quantitative determination of the various elements was made from XPS spectra. Relative concentrations were normalised to the silver content and reported as a function of operation time in a chlor-alkali cell.

Figure 12 shows the variation of relative XPS concentrations for the various elements versus operation time. The atomic ratio of F/Ag and C/Ag decreased with time while O/Ag increased. This means that hydrophobicity decreased and the amount of hydroxides increased. The most significant variation in surface properties occured in the first period of operation. A drastic decrease is observed in Hg in the first 50 h according to the EDX analysis. The precipitation of sodium hydroxide and AgCl is also confirmed by the plot of Na and Cl concentrations normalized to Hg versus time (Fig. 13). As observed above, it seems that the formation of hydroxides prevails with respect to AgCl.

Interestingly, the decrease in Hg content from the inner layers (Fig. 14a), as determined by XPS analysis of the sputtered electrodes, is not as drastic as that observed in the outer layers by both XPS and EDX. This indicates that there is a progressive migration of Hg from the bulk to the surface, followed by dissolution into the electrolyte. The precipitation of sodium hydroxide and AgCl is observed in the XPS data on sputtered electrodes (Fig. 14b).

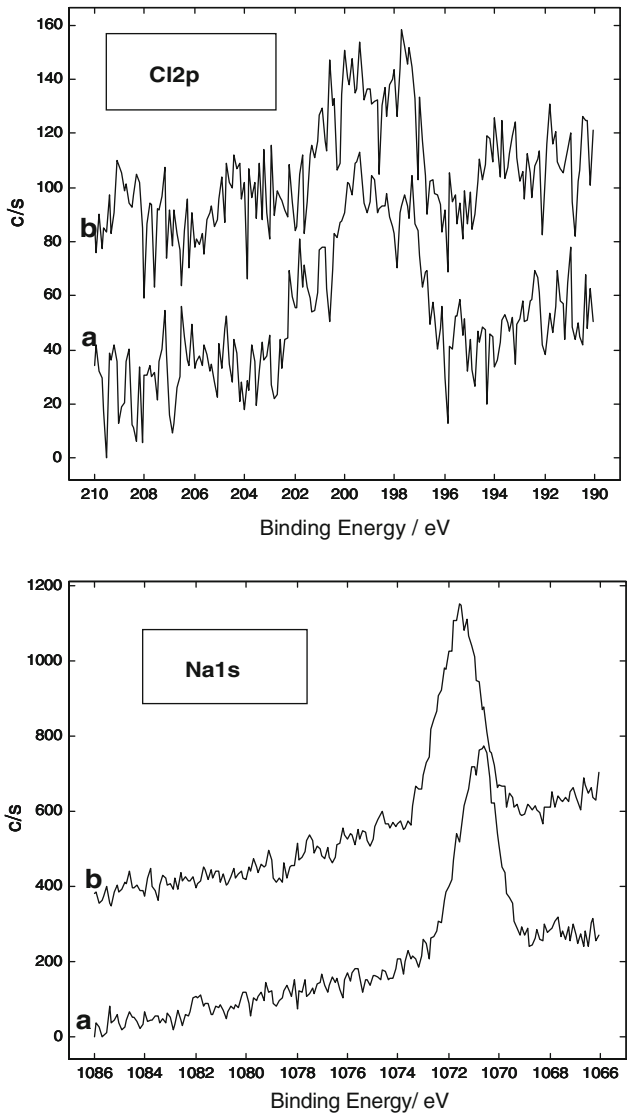

Fig. 9 Cl 2p and Na 1 s XPS spectra of GDE-1, before (**a**) and after (**b**) sputtering

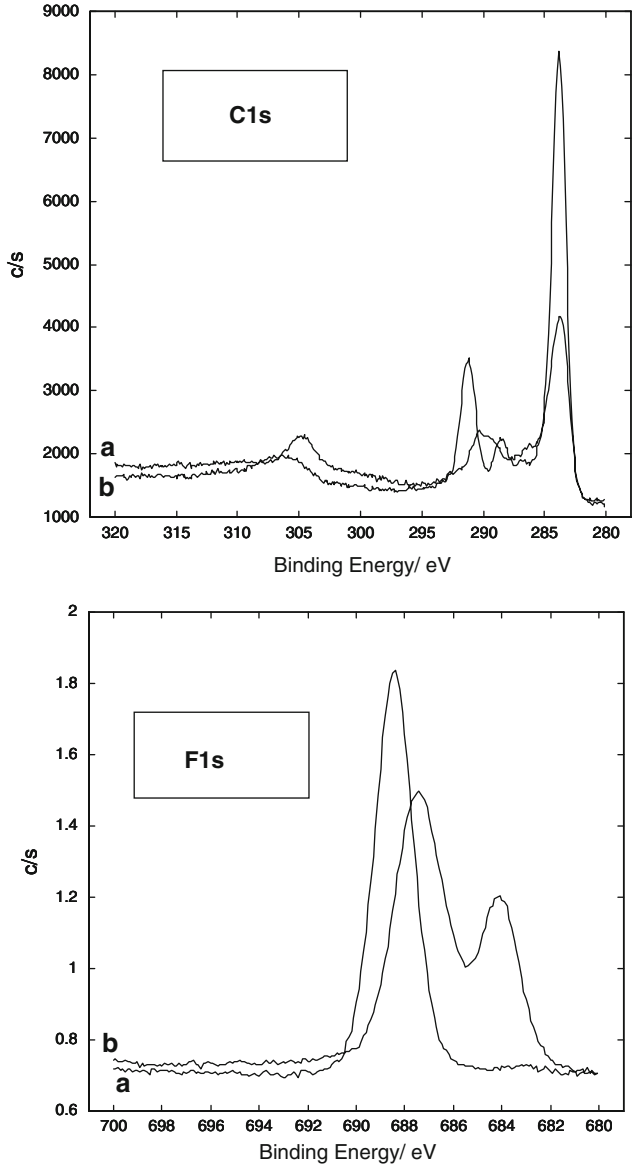

Fig. 10 C 1 s and F 1 s XPS spectra of GDE-2, before (**a**) and after (**b**) sputtering

Careful observation of electrodes by SEM and EDX allowed the identification of local formation of sodium hydroxide, AgCl, and Hg particles on the surface resulting from precipitation and Hg segregation, respectively. This is a qualitative confirmation of what is derived from EDX and XPS analyses (Fig. 15).

Figure 16a shows a comparison of mass change versus temperature in GDE-fresh, GDE-1, and GDE-2. The result of thermal analysis carried out on the electrodes discharged after 526 h were similar to those of electrodes discharged after 145 h.

The TG-DSC analysis of the various electrodes allowed the identification of three main mass-change regions associated with a loss of volatile compounds (up to 150 °C), PTFE degradation (up to 320 °C), and an Hg loss in bulk (Fig. 16a). The Hg loss in the thermal analysis experiments decreased progressively as a function of operation time, indicating a reduction of Hg content in electrodes as the length of time of operation in a chlor-alkali cell increases (Fig. 16b). This is a further confirmation that Hg diffuses from the bulk to the interface, segregating on the surface as observed by SEM; subsequently, it dissolves into the solution.

Previous studies concerning the use of oxygen cathodes in chlor-alkali cells have shown there is a high potential of reducing the power requirements of these devices [10]. Life-time operation of more than 1200 days has been demonstrated for carbon black supported Ag electrodes. Cell voltages between 2.2 and 2.4 V @ 3 kA m^{-2} were observed for Ag loading as small as 2.6 mg cm^{-2} [10]. The

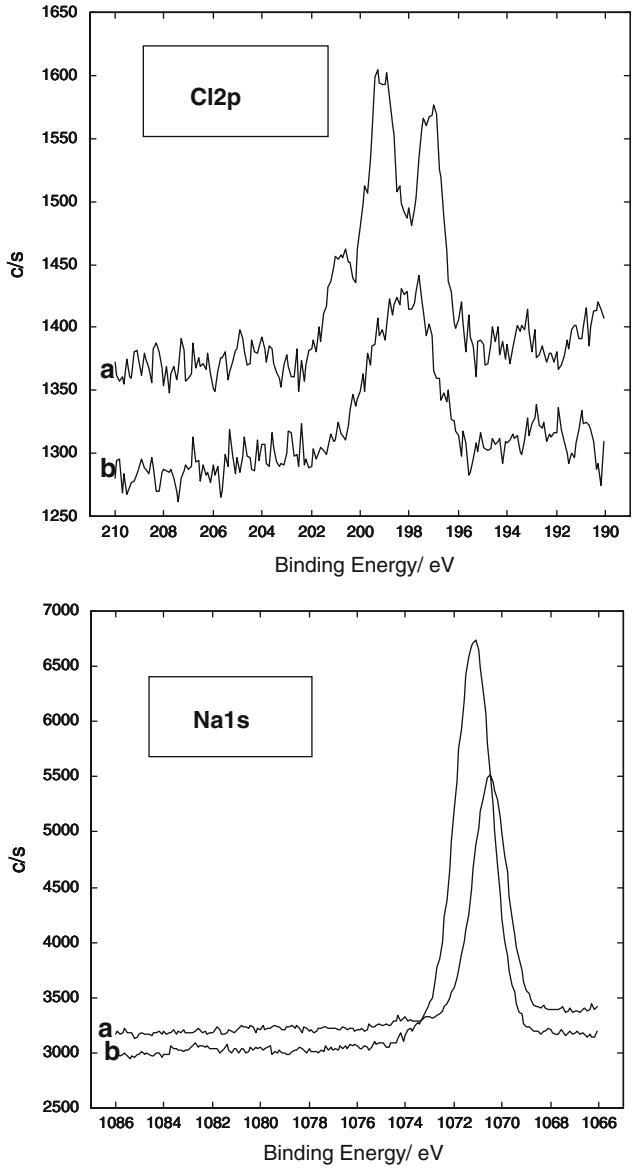

Fig. 11 Cl 2p and Na 1 s XPS spectra of GDE-2, before (**a**) and after (**b**) sputtering

role of Ag in the ORR in a 32% NaOH electrolyte at 80 °C was attributed to the promotion of the four-electron oxygen reduction to OH^- while avoiding H_2O_2 as reaction intermediate [8].

In our experiments we recorded cell voltages of 2 V @ 3 kA m^{-2} but only in the presence of a large excess of Ag catalyst. This catalyst layer differs from the carbon supported Ag catalysts previously reported in the literature on large Ag loading and Hg addition. Large Ag loading allows the proper protection of a current collector and ensures long-term stability. This reaction occurs at the interface with the electrolyte; thus, only a small fraction of the total amount of Ag is involved in the electrochemical process. Despite higher costs, this approach reduces the risks of

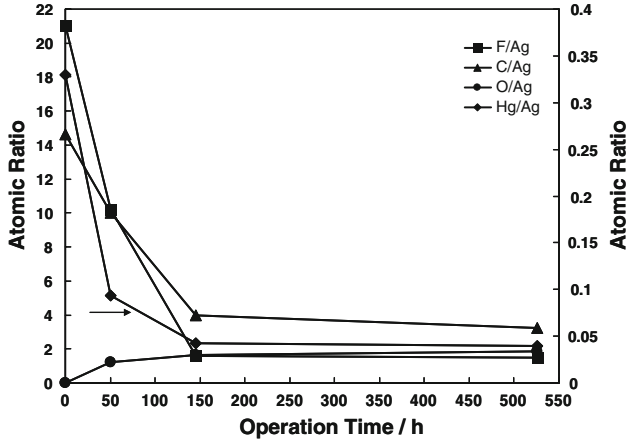

Fig. 12 Comparison of relative concentrations for GDE-fresh, GDE-1, GDE-2 and GDE-3 electrodes derived from XPS before sputtering

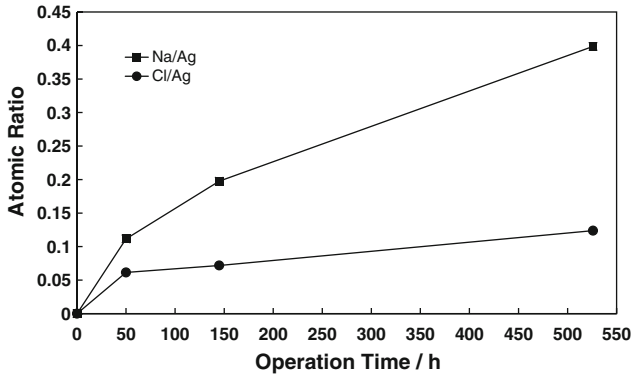

Fig. 13 Variation of Na/Ag and Cl/Ag ratios versus operation time as derived from XPS

process interruption over several years of operation. From previous reports on fuel cells [16], we preferred to avoid a carbon support since it is oxidized to CO_2 by the oxygen feed over long periods of operation. This usually causes irreversible degradation of the catalyst. Hg is reported to stabilize Ag against corrosion [12]. However, the present analysis shows that this protection is less effective during the first period of operation, in which Hg migrates towards the surface causing a small segregation. This phenomenon, is possibly responsible for a rapid increase in overpotential at the beginning of electrochemical testing. Yet, it does not continue as significantly over time as revealed by our physico-chemical analyses. After the first 40 h, cell voltage shows only a small, steady decay over time. The present physico-chemical analysis shows a small loss in hydrophobicity with time. This improves the wetting properties of the catalyst surface but causes constraints on oxygen mass transport at the interface.

Electrodes prepared in accordance with this approach show the capacity to operate for two decades in chlor-alkali cells; however, it is imperative to reduce the initial decay

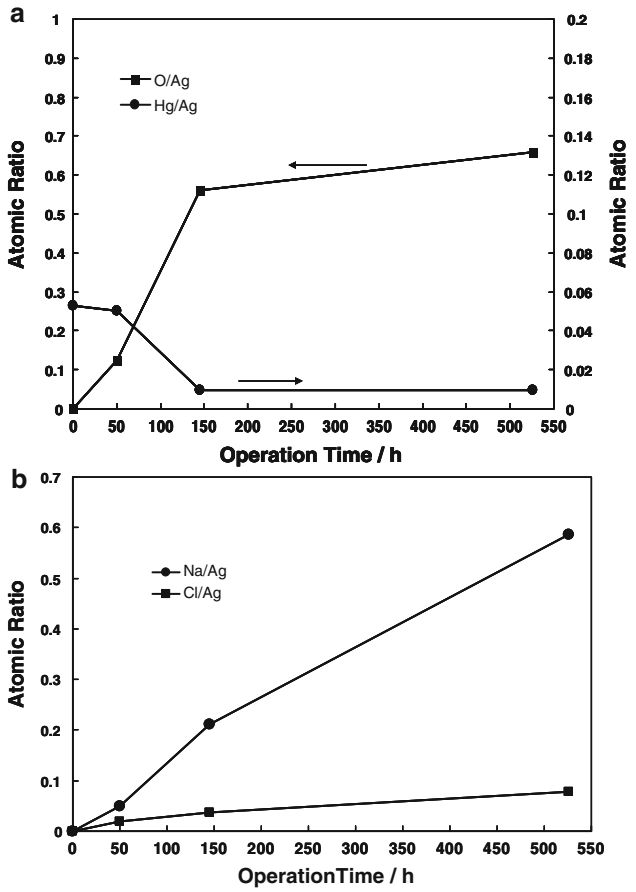

Fig. 14 Qualitative comparison among GDE-fresh, GDE-1, GDE-2 and GDE-3 versus atomic ratio of different elements using XPS after sputtering: (**a**) O/Ag and Hg/Ag; (**b**) Na/Ag and Cl/Ag

that affects overall performance. The identification of the constraints that determine cell voltage increase versus time is the first step towards this goal.

4 Conclusions

The purpose of the present study was to investigate the cathodic properties for the oxygen reduction at gas-diffusion electrodes (GDEs) for electrolysis in chlor-alkali cells at 90 °C.

Gas diffusion electrodes were analysed before and after different operation times in a chlor-alkali cell. Electrode stability was investigated by life-time tests. The surface of gas diffusion electrodes was analyzed for both fresh and used cathodes by scanning electron microscopy (SEM-EDX) and X-ray photoelectron spectroscopy (XPS). The bulk of gas diffusion electrodes was studied by X-ray diffraction (XRD) and thermogravimetric analyses (TG-DSC). Two main degradation processes occurring on different time-scales have been identified and attributed to a segregation and loss of Hg at the interface and a decrease in

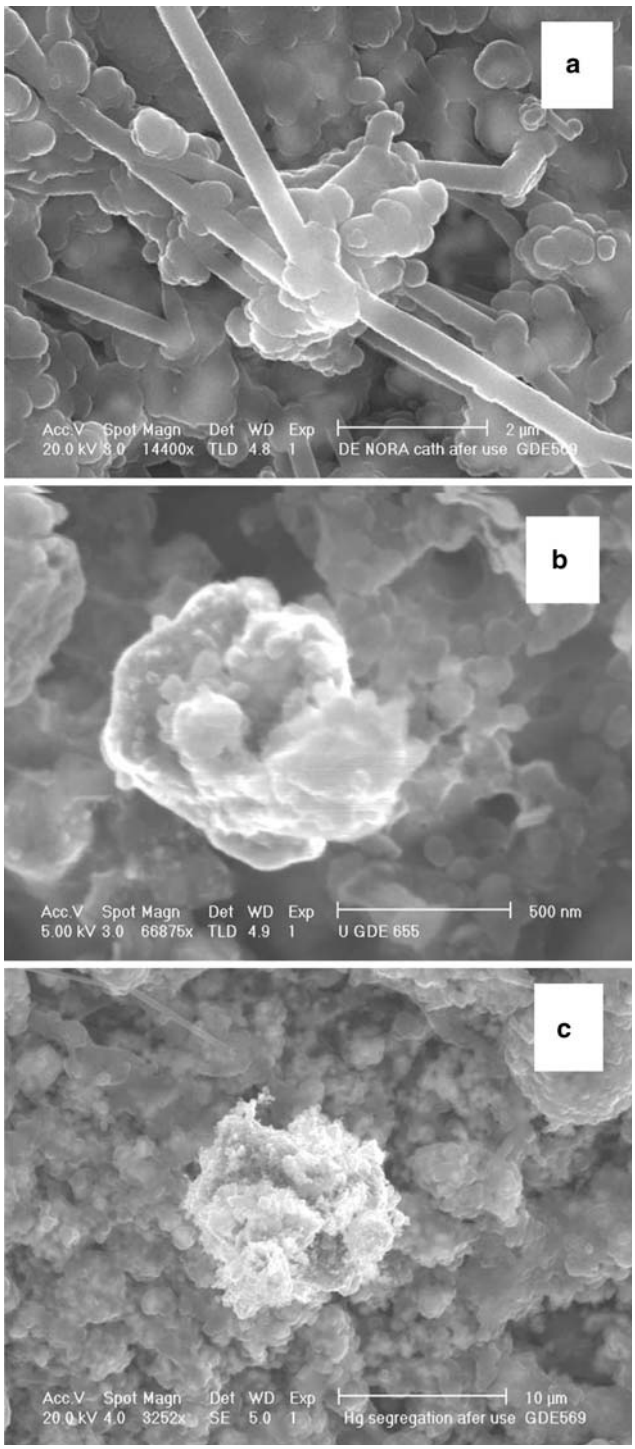

Fig. 15 SEM pictures of the electrode surface: (**a**) panoramic view of the electrode surface evidencing PTFE fibres; (**b**) evidence of sodium hydroxide particle; (**c**) Evidence of Hg particles segregated in the surface

hydrophobic properties with time. The Hg loss at the interface was identified in both EDX and XPS analyses and qualitatively observed by SEM. This process is quite significant in the first 50 h of operation. The dramatic

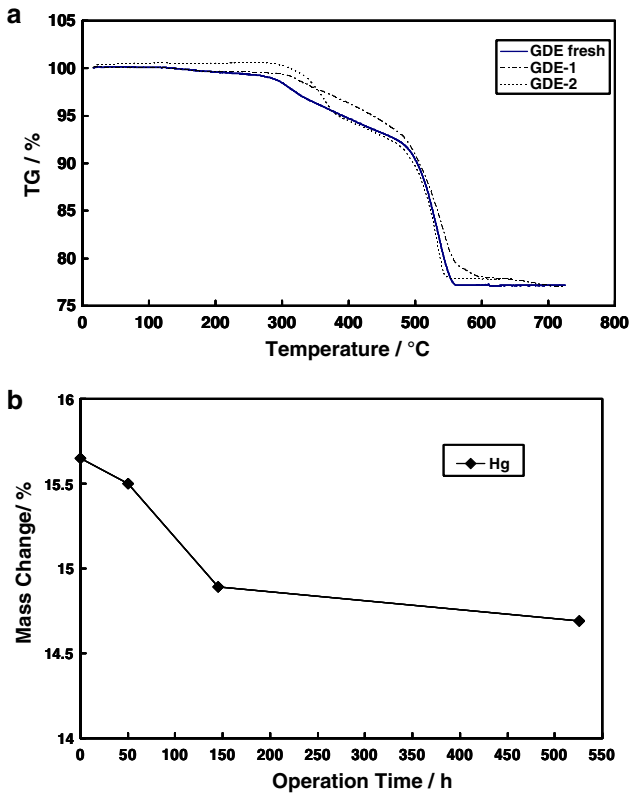

Fig. 16 (**a**) TG-analysis of GDE-fresh, GDE-1 and GDE-2. (**b**) Hg mass change in the bulk versus operation times

(logarithmic) increase in overpotential is most likely associated with Hg segregation on the surface and dissolution at the interface. Subsequent to the first 50 h, this process proceeds less rapidly with time, involving a slow migration from the bulk (TG analysis). The decrease in hydrophobic properties occurs progressively during all periods of operation as evidenced by EDX and XPS analyses and qualitatively corroborated by TEM. This latter process, together with progressive Hg loss from the bulk, could be associated with the linear decay on a large timescale. Furthermore, an increase in the precipitation of products from the reaction process also contributes to a decrease in performance resulting from the occlusion of reaction pores. Such an effect should influence, primarily, mass transport properties at high current densities. The effects of this phenomenon are not clearly envisaged from the electrochemical experiments carried out at practical current densities. These phenomena may cause electrode blocking after prolonged operation. There is no significant change in the particle size of the catalysts at different intervals of operation; this indicates that the degradation of electrodes is not associated with any electrochemical sintering of the catalysts.

References

1. Faita G, Federico F (2002) European Patent 1362133
2. Gritzner G (1977) US Patents 4 035 254 and 4 035 255
3. Gestaut L et al. (1983) abstracts of ECS Fall Meeting, No. 393
4. Aikawa H, Poblotzki J (1996) Soda and Chlorine 47:93
5. Gestaut LJ, Clere TM, Niksa AJ, Graham CE (1983) The Electrochemical Society Extended Abstracts, Abstract 124:196, vol. 83-2. Los Angeles, CA, May 8–13 1983
6. Chatenet M, Aurousseau M, Durand R, Andolfatto F (2003) J Electrochem Soc 150:D47
7. Uchimura A, Ichinose O, Furuya N (1997) Denki Kagaku 65:1032
8. Ichinose O, Kawaguchi M, Furuya F (2004) J Appl Electrochem 34:55
9. Aikawa H, Poblotzki J (1994) Sodium Hydroxide Enso 45:85
10. Furuya N, Aikawa H (2000) Electrochim Acta 45:4251
11. Janowitz K, Dresel T, Woltering P (2004) US Patent 2004/0152588 A1
12. Nidola A (1980) In: Trasatti S (ed) Electrodes of conductive metallic oxides, part B,–Chapter 11–Technological impact of metallic oxides as anodes. Elsevier Scientific Publishing Company, p 646
13. Martelli GN, Ornelas R, Faita G (1994) Electrochim Acta 39(11/12):1551
14. Martelli GN, Reduzzi E, Caldarera A, Urgeghe C (2004) Joint International Meeting. The Electrochemical Society Inc., Honolulu, Hi, USA, October 3–8 2004
15. Staiti P, Aricò AS, Antonucci V, Hocevar S (1998) J Power Sources 70:91
16. Ball SC, Hudson SL, Thompsett D, Theobald B (2007) J Power Sources 171(1):18